Microemulsion Polymerization. 2. Influence of Monomer Partitioning, Termination, and Diffusion Limitations on Polymerization Kinetics

Renko de Vries, Carlos C. Co, and Eric W. Kaler*

Center for Molecular and Engineering Thermodynamics, Department of Chemical Engineering, University of Delaware, Newark, Delaware 19716

Received July 18, 2000; Revised Manuscript Received January 2, 2001

ABSTRACT: We investigate the polymerization kinetics of microemulsions prepared with the cationic surfactant dodecyltrimethylammonium bromide and the hydrophobic monomers *n*-butyl methacrylate, *tert*-butyl methacrylate, *n*-hexyl methacrylate, and styrene. Our previous model for microemulsion polymerization kinetics cannot account for the kinetics of these systems**.** Using the results of small-angle neutron scattering monomer partitioning studies and an extended kinetic model to analyze the data, the failure of the original kinetic model is shown to be due to a combination of nonlinear monomer partitioning, nonnegligible bimolecular termination, and, in some cases, diffusion limitations to propagation.

1. Introduction

In the first paper of this series we investigated the thermodynamics of polymerizing microemulsions. The monomer concentration in polymer particles formed during microemulsion polymerization was determined using small-angle neutron scattering (SANS), and a simple thermodynamic monomer partitioning model was developed that explains our experimental findings.

These results set the stage for the present paper, the aim of which is to develop a better understanding of the kinetics of microemulsion polymerization of hydrophobic monomers initiated with water-soluble initiators. A number of attempts have already been made at modeling the microemulsion polymerization kinetics for these systems,[1−6] but as yet there is no generally applicable model. Models that have been proposed each address a specific system.

An elaborate model for the kinetics of styrene microemulsion polymerization has been proposed by Guo et al.[5] This model accounts for the observed kinetics up to fairly high conversions but fails to describe the observed growth of the particle number density. To account for the experimentally observed kinetics, the model requires that the rate constant for the capture of an aqueous phase free radical by a monomer-swollen micelle is many orders of magnitude smaller than that for capture by a polymer particle. A very similar model was recently proposed by Mendizabal et al.[6]

We have previously studied the microemulsion polymerization of *n*-hexyl methacrylate (C_6MA) in microemulsions prepared using a mixture of dodecyltrimethylammonium bromide (DTAB) and didodecyldimethylammonium bromide (DDAB) surfactants.[1−4] A simple kinetic model was developed,[2] and solved analytically, based on the simplifying assumptions that bimolecular termination is negligible and that the monomer concentration in the growing particles decreases linearly with increasing conversion. With these assumptions, a rate maximum is predicted to occur at 39% conversion, independent of any characteristic of the system, in good agreement with our experimental observations. Moreover, full quantitative agreement between theory and experiment was found for all conversions, using literature values for the various parameters.

Previously we have suggested that in some cases the failure of our simple kinetic model[2] may be due to the pH dependence of the initiation efficiency[7] of unbuffered persulfate initiators that are typically used. However, for styrene microemulsion polymerizations initiated with the pH-insensitive cationic initiator 2,2′-azobis(2-amidinopropane) hydrochloride (V50), it was found that the rate maximum still occurs at ∼20%. Similarly, rate maxima at conversions significantly below 39% have been found for a number of other systems initiated with V50 and buffered persulfate initiators. Hence, while pH effects may be important in some cases, they are not the only cause of the observed differences.

Instead, it is more likely that the failure of our original kinetic model for systems other than the base case of C_6MA/DTAB/DDAB microemulsions is due to nonnegligible bimolecular termination, nonlinear monomer partitioning, or diffusion-limited propagation due to glass transition. In part 1 of this series, we have shown that monomer partitioning may be significantly nonlinear. However, as it turns out, nonlinear monomer partitioning alone is insufficient to explain the failure of our previous kinetic model for styrene microemulsion polymerizations. This suggests that termination and/or diffusion limitations may also be important.

Here, we study the polymerization kinetics of *n*-butyl methacrylate (nC_4MA), *tert*-butylmethacrylate (tC_4MA), C_6MA, and styrene microemulsions prepared with DTAB. We have previously studied the monomer partitioning behavior of these four systems in part 1 of this series. The choice of these monomers allows us to independently probe the effects of monomer water solubility, polymer glass transition temperature, and propagation rate constant on the polymerization kinetics. We also extend our previous kinetic model by including both the observed nonlinear monomer partitioning and accounting for the possibility of bimolecular termination. Using the extended kinetic model to analyze the data, we demonstrate that for nC_4MA and C_6MA microemulsions the failure of our previous kinetic model is due to

* Corresponding author. Tel (302) 831-3553; Fax (302) 831-8201; E-mail kaler@che.udel.edu.

10.1021/ma001247j CCC: $20.00
Published on Web 04/10/2001

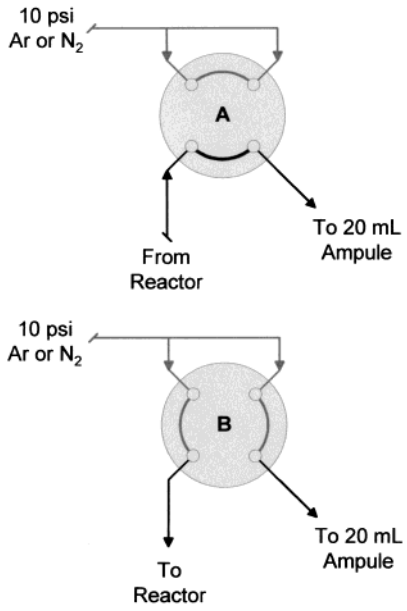

Figure 1. Sample withdrawal system used in measuring polymerization kinetics. In position A, the sample is withdrawn directly into 20 mL ampules for gravimetric analysis. In position B, the residue in the sampling lines are flushed.

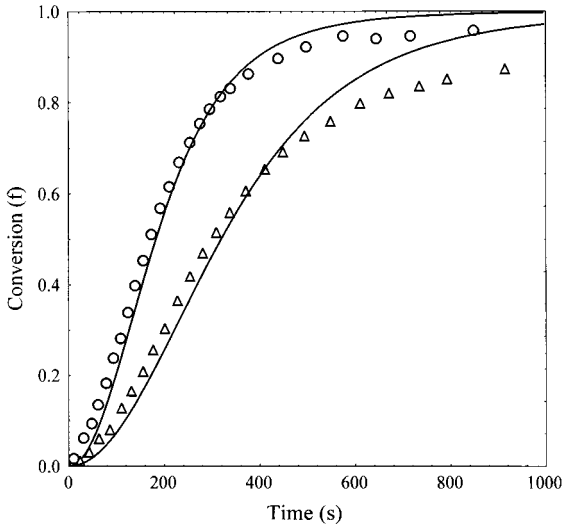

Figure 2. Experimental and model calculated kinetics for C_6-MA/DTAB microemulsions initiated with varying concentrations of V50: (○) 0.044 mM and (□) 0.015 mM that correspond respectively to 0.045 and 0.015 wt % relative to the amount of monomer in the microemulsion.

nonlinear monomer partitioning. For styrene microemulsions, we argue that bimolecular termination cannot be neglected. In addition, diffusion limitations to propagation may be important for both tC_4MA and styrene microemulsion polymerizations even at low conversions.

We consider chemical initiation by water-soluble initiators only. Initiation by oil-soluble initiators is more complicated. The radical pair that presumably forms in either the micelles or in the polymer particles may either recombine or the radicals may exit the micelles or particles in a way that is expected to depend sensitively on the micelle and particle properties. This complication is absent for water-soluble initiators.

2. Materials and Methods

All monomers (nC_4MA, tC_4MA, C_6MA, and styrene) were purchased from Scientific Polymer and vacuum distilled to remove inhibitors. The distilled monomers were stored in a freezer for less than 5 days before use. DTAB (99+%) from TCI and V50 initiator (98.8%) provided by Wako were used as received. Prior to preparing the microemulsions, deionized water (18.3 MΩ cm) was boiled under vacuum for at least 30 min, and the monomers were sparged with ultrahigh-purity N_2 (<1 ppm of O_2) for 15 min to remove oxygen and then sealed. Thirty grams of DTAB was weighed into a 500 mL water jacketed reactor equipped with a stirrer, condenser, and heated reactor head. The reactor was sealed and then purged thoroughly with four cycles of vacuum and ultrahigh-purity N_2. The deoxygenated water and monomers (212.4 and 6.6 g, respectively) were then injected into the reactor. This composition corresponds to a surfactant weight fraction (γ) of 12 wt % and a monomer weight fraction on a surfactant-free basis (α) of 3 wt %. After heating to 60.0 °C, polymerization of the microemulsion was initiated by injecting 1 g of a V50 solution prepared using deoxygenated water. After an induction period of less than 30 s, the microemulsions became faintly bluish, indicating the onset of polymerization.

Over the course of the reaction, ~5 mL samples are taken out from the reactor directly into preweighed 20 mL ampules using the sampling valve shown in Figure 1. The ampules are immediately sealed with a septa and then frozen in liquid nitrogen. Exposure to oxygen instantaneously quenches the sample as it enters the ampules, and freezing in liquid nitrogen is done only as a precaution. Even when kept at 60 °C for an additional 30 min, no additional polymerization can be detected in the sealed samples that have been exposed to oxygen. Condensate on the exterior of the ampules is washed off with acetone, and then the amount of sample in the ampules is measured by difference. Water and monomer are evaporated by positioning the ampules horizontally overnight under a gently blowing air stream. A volatile solvent (e.g., acetone) in which the surfactant is insoluble is then used to extract residual volatiles from the cake, and the ampules are air-dried again after rotating them 180° in the rack. After thorough air-drying, the samples are dried further in a vacuum oven initially kept at 30 °C for 12 h and then ramped up to 60 °C for 6 h. The samples are cooled to ambient temperature and then reweighed. The weighings are performed carefully on a four-digit balance, and the precision of the 30−40 conversion measurements obtained for each reaction is routinely better than ±0.5%. The accuracy of these measurements is within ±1% and is limited by the accuracy in preparing the original microemulsion.

To extract rates of polymerization, the conversion vs time data are differentiated using Craven and Wahba's cross-validation smoothing spline algorithm.[8] Statistical validity is then examined using a bootstrapping algorithm[9] to account for experimental errors in measuring both conversion and time. For each iteration of this bootstrapping procedure, all data points are resampled from normal distributions centered around the original data points with standard deviations of 1 s and 0.5% respectively for the time and conversion. The resampled data set is then differentiated using the cross-validation smoothing spline algorithm after which the rates at a few randomly chosen conversions are recorded together with the position of the rate maximum. One thousand iterations of this bootstrapping procedure are performed for each data set to obtain error estimates for the position of the maximum rate of polymerization. The large set of rates recorded at random conversions are then plotted, e.g., Figure 3, to permit a qualitative assessment of the agreement between theory and experiment.

The aqueous solubilities of the monomers at 60 °C were measured using UV absorbance. Samples containing deionized water and a slight excess of vacuum distilled monomer were equilibriated and then allowed to phase separate over 4 h at 60.0 °C. Approximately 10 g of the aqueous phases was taken directly into syringes containing ~10 g of ethanol. The monomer concentration was then measured by monitoring the UV absorption at 205 and 220 nm for nC_4MA, tC_4MA, and C_6-

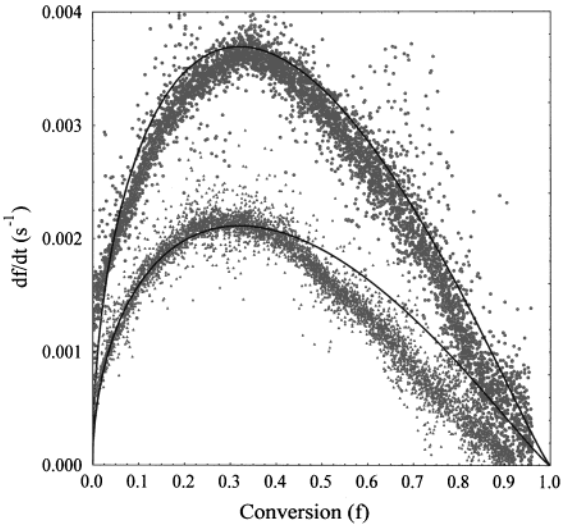

Figure 3. Experimental and model rate vs conversion profiles obtained by differentiating the data shown in Figure 2.

Table 1. Monomer Physical Properties

	C_6MA	nC_4MA	tC_4MA	styrene
water solubility at 60 °C (mM)	~0.4[a]	3.4[a]	4.3[a]	4.6[b]
T_g (°C)	−5[20]	20[20]	128	106
k_p at 60 °C (M^{-1} s^{-1})	995[28]	1015[28]	1140[33]	342[34,35]

[a] Measured as described in section 2. [b] Interpolated from data by Lane.[10]

MA and at 203 and 248 nm for styrene. Linear calibration curves were obtained using standard solutions with the same water/ethanol ratio as the unknown. The styrene aqueous solubility of 4.6 ± 0.3 mM shown in Table 1 is in agreement with the value of 5.1 mM obtained by interpolating measurements done by Lane.[10] Likewise, our measurement of 3.4 ± 0.3 mM for the aqueous solubility of nC_4MA at 60 °C is consistent with the value of 2.5 mM at 50 °C as measured by Gilbert et al.[11] The aqueous solubility of C_6MA is low and hampers the reproducibility of our measurements. We estimate an aqueous solubility of ~0.4 mM for C_6MA that is also consistent with group contribution estimates.[12]

The glass transition temperatures of microemulsion polystyrene and poly-tC_4MA were measured using a Perkin-Elmer DSC7, at heating rates of 20 and 10 °C/min. Latexes of polystyrene and poly-tC_4MA were precipitated and washed repeatedly with an excess of methanol and vacuum-dried at 40 °C. Just as Quian et al.[13] have observed, an exotherm was recorded at the approximate glass transition temperature during the initial scan of both polymers. Subsequent scans did not exhibit this release of energy that is related to the kinetically controlled conformation of the polymers as discussed by Quian et al.[13] The glass transition reported in Table 1 are those measured for a heating rate of 10 °C/min, which are ~1.5 °C less than that measured at a heating rate of 20 °C/min.

3. Theory

This section briefly reviews our previous kinetic model that is now extended to account for nonlinear monomer partitioning and termination. We also briefly discuss possible diffusion limitations to propagation for tC_4MA and styrene microemulsion polymerizations.

The basic sequence of events has been outlined in our previous papers.[2,3] After adding a water-soluble initiator to the microemulsion, primary free radicals are generated in the aqueous phase at a rate ρ_0,

$$\rho_0 = 2k_d[I] \tag{1}$$

where [I] is the initiator concentration and k_d is the first-order rate constant for initiator decomposition. The reaction of a primary free radical ($I^\bullet$) with a first monomer (M) is reported to occur very rapidly, essentially in the diffusion-limited regime.[14] The resulting species ($IM^\bullet$) either may be amphiphilic enough to directly enter a monomer-swollen micelle and start propagating or require further propagation steps in the aqueous phase. This is mechanistically similar to the Maxwell−Morisson model[15] for radical entry in emulsion polymerizations. If aqueous phase propagation is necessary, the free radical concentration may build up to levels where aqueous phase termination can no longer be neglected.

Chain growth may stop by either bimolecular termination or chain transfer to monomer. In view of the high concentration of surfactants, particle coalescence is expected to be negligible, and bimolecular termination by this mechanism can be excluded. Because of the small particle sizes, microemulsion polymerization is expected to obey zero-one kinetics. Therefore, the main mode of bimolecular termination for growing chains in microemulsion polymerization is the entry of a second free radical into a growing particle, followed by instantaneous termination. Monomeric radicals ($M^\bullet$) generated by chain transfer to monomer may either continue propagating in the same particle or exit to the aqueous phase. For the small particles produced by microemulsion polymerization, exit is by far the most probable fate of the transfer-generated ($M^\bullet$) molecules.

The fundamental equation for the rate of the microemulsion polymerization reaction is

$$\frac{\partial f}{\partial t} = \frac{k_p C_{mon}^{(part)} N^*}{M_0} \tag{2}$$

This assumes a negligible contribution from aqueous phase propagation. In eq 2, f is the fractional conversion, M_0 is the initial concentration of monomer in moles per liter of microemulsion, k_p is the propagation rate constant, $C_{mon}^{(part)}$ is the monomer concentration at the locus of polymerization in the growing polymer particles, and N^* is the concentration of propagating radicals. Note that, in view of our assumption of zero-one kinetics, N^* also equals the concentration of growing particles. Except for M_0, all of the quantities on the right-hand side of eq 2 may vary as the reaction proceeds. The propagation rate constant k_p varies significantly only if the polymer passes through a glass transition during the reaction, in which case the reaction becomes limited by diffusion rather than reaction. In the absence of a glass transition, k_p is approximately constant.

The concentration of monomer in the growing particles, $C_{mon}^{(part)}$, is determined by how the unreacted monomer partitions between the polymer particles and the large number of coexisting surfactant micelles. We have previously assumed that for C_6MA/DTAB/DDAB microemulsion polymerization monomer partitioning is linear,[2−4]

$$C_{mon}^{(part)} = C_{mon,0}^{(part)}(1 - f) \tag{3}$$

Next, consider the concentration of growing particles, N^*. For microemulsion polymerization the ratio of N^* to the total number density of dead polymer particles

and monomer-swollen micelles N is[4,16]

$$\frac{N^*}{N} \approx 10^{-4}-10^{-3} \tag{4}$$

where, to a very good approximation, N equals the concentration of monomer-swollen micelles. Therefore, we have previously argued that the entry of an aqueous phase free radical into a growing particle is a highly improbable event. The capture of aqueous phase, initiator-derived free radicals by monomer-swollen micelles can be assumed to be a process that is fast on the time scale of the polymerization reaction, even if capture requires some aqueous phase propagation. The explicit rate equation for the concentration of aqueous phase, initiator-derived free radicals can therefore be eliminated using the steady-state approximation. Neglecting termination in the particles, the rate equation for N^* can then be written as

$$\frac{\partial N^*}{\partial t} = \rho \tag{5}$$

where $\rho = \gamma_{\text{eff}}\rho_0$, and γ_{eff} is an efficiency factor, assumed to be independent of conversion, that accounts for possible aqueous phase termination. Note that, in the absence of termination, chain transfer to monomer does not affect the total number of growing particles and hence does not appear in eq 5. Combining eqs 2 and 5 we find

$$\frac{\partial f}{\partial t} = A(1 - f)t \tag{6}$$

$$A = \frac{k_p C_{\text{mon},0}^{(\text{part})}\rho}{M_0} \tag{7}$$

the solution of which is

$$f(t) = 1 - \exp\left(-\frac{1}{2}At^2\right) \tag{8}$$

This has a rate maximum at $t = A^{-1/2}$, at a conversion of $f = 1 - e^{-1/2} \approx 0.39$.[2] For microemulsion polymerizations of C_6MA in mixed DTAB/DDAB microemulsions, we have demonstrated that eq 8 quantitatively accounts for the polymerization kinetics for reasonable values of the various parameters, assuming negligible aqueous phase termination, $\gamma_{\text{eff}} = 1$. Rate maxima at ~40% conversion have also been reported by Capek and Juranicova[17] for the microemulsion polymerizations of ethylhexyl methacrylate. Reanalysis of the kinetic data by Full et al.[18] for tetrahydrofurfuryl methacrylate microemulsions also reveals a rate maximum at ~40% conversion. Note that in both cases the monomers have very low water solubilities and low polymer glass transition temperatures. However, all other systems that have been studied so far seem to have rate maxima at conversions significantly below 40%, for reasons that will now be explored.

3.1. Nonlinear Monomer Partitioning. To test the assumption of linear monomer partitioning, in part 1 of this series, we have studied monomer partitioning in polymerizing microemulsions. These monomer partitioning results are correlated by the empirical interpolation formula

$$C_{\text{mon}}^{(\text{part})} = C_{\text{mon},0}^{(\text{part})}(1 - f)^b \tag{9}$$

Table 2. Conversion at the Maximum Rate of Polymerization (f_{max}) for Varying Values of the Kinetic Model Exponent (b) in Eq 10

b	f_{max} (%)
1	39
1.2	35
1.4	32
1.6	29

Only for a styrene microemulsion with low monomer content ($\alpha = 3$ wt %) far away from the phase boundary ($\alpha = 8.2$ wt %) did we find linear monomer partitioning ($b \approx 1$). For other microemulsions with compositions closer to the phase boundary, monomer partitioning was significantly nonlinear ($b \approx 1.4$).

If bimolecular termination can still be neglected, the equation for the rate of polymerization, now accounting for nonlinear monomer partitioning, can be written as

$$\frac{\partial f}{\partial t} = A(1 - f)^b t \tag{10}$$

with A again given by eq 7. The conversion at the maximum rate is now a function of the exponent b, and increasing b from 1 to 1.6 lowers the location of the maximum from 39% to 29% (Table 2). Hence, nonlinear monomer partitioning can indeed account for a shift of the location of the rate maximum to lower conversions. However, for $b = 1.4$, as found in our experiments, the maximum only shifts down to 32%, which is still much larger than the typical value of ~20% observed for styrene microemulsion polymerization. Therefore, we proceed to also consider the possibility of bimolecular termination.

3.2. Termination in the Particles. Previously, we have argued that termination should be negligible for microemulsion polymerization[2] in view of the large excess of micelles over growing polymer particles, as expressed by eq 4. Such an argument would indeed hold if the small aqueous phase free radicals, including both the initiator-derived and the transfer-generated radicals, always start propagating upon entering or adsorbing on a monomer-swollen micelle. However, this surely depends on the reactivity of these radicals. Free radicals that are still small enough to have some aqueous phase solubility could enter and exit a large number of swollen micelles before eventually propagating in one. This would greatly enhance the probability for them to encounter and terminate a growing polymer particle. Following the discussion of Maxwell et al.[15] for emulsion polymerization, this is easily understood considering the time scales involved. The typical time scale for propagation in a monomer-swollen micelle is

$$\tau_{\text{prop}} = (k_p C_{\text{mon}}^{(\text{mic})})^{-1} \tag{11}$$

so for $k_p \approx 10^3$ M^{-1} s^{-1} and $C_{\text{mon}}^{(\text{mic})} \sim 1$ M, $\tau_{\text{prop}} \approx 10^{-3}$ s.

There are two types of aqueous phase small free radicals: initiator-derived radicals ($IM_n^{\bullet}$) and monomeric free radicals ($M^{\bullet}$) generated by chain transfer to monomer. For water-soluble initiators, the initiator-derived small free radicals are surfactant-like molecules. Typical residence times of surfactants in micelles ($\tau_{\text{res}} \approx 10^{-6}-10^{-5}$ s) depend strongly on their aqueous monomeric solubility. Similar residence times may be expected for small initiator-derived free radicals. An estimate of the residence time for transfer-generated

monomeric radicals ($M^{\bullet}$) in monomer-swollen micelles is[15]

$$\tau_{res} \approx q \frac{R_{mic}^2}{3D_{mon}^{(aq)}} \tag{12}$$

where $R_{mic} \approx 3$ nm is the micelle radius, $D_{mon}^{(aq)} \approx 10^{-9}$ $m^2\ s^{-1}$ is the diffusion constant of the monomer in the aqueous phase, and $q \approx 10^3-10^4$ is the partition coefficient of the monomer between the micelles and the aqueous phase. For these values, $\tau_{res} \approx 3 \times 10^{-6}-3 \times 10^{-5}$ s.

Therefore, an aqueous phase free radical will typically adsorb on and desorb from 10^2-10^3 monomer-swollen micelles before propagating. Recalling that the ratio of the number of monomer-swollen micelles to growing particles is 10^3-10^4, it becomes clear that there is indeed a nonnegligible probability that small free radicals in the aqueous phase might terminate growing particles during microemulsion polymerization.

To develop a rate equation for the number of growing particles that includes the possibility of termination via the above mechanism, let p_{prop} be defined as the probability that, after a single adsorption−desorption step, the oligomeric free radical has propagated in a monomer-swollen micelle. Likewise, p_{term} is the probability that, after a single adsorption−desorption step, the oligomeric free radical has terminated a growing particle. In view of the discussion above, p_{prop} and p_{term} are both much less than unity. After infinitely many adsorption−desorption steps, the probability that the oligomeric free radical will have propagated is $P_{prop} = p_{prop}/(p_{prop} + p_{term})$. The probability that the oligomeric will have terminated a growing particle is $P_{term} = 1 - P_{prop}$. Thus, a more complete rate equation for the number of growing particles that accounts for termination is

$$\frac{\partial N^*}{\partial t} = \rho(P_{prop} - P_{term}) - 2k_{tr}C_{mon}^{(part)}N^*P_{term} \tag{13}$$

$$= \rho \frac{1 - p_{term}/p_{prop}}{1 + p_{term}/p_{prop}} - 2k_{tr}C_{mon}^{(part)}N^* \frac{p_{term}/p_{prop}}{1 + p_{term}/p_{prop}} \tag{14}$$

In more physical terms, these equations describe the following: Initiator-derived small free radicals are generated at a rate ρ. A fraction P_{prop} of these eventually propagate in a monomer-swollen micelle, each increasing the number of growing particles by one. The remaining fraction P_{term} terminate growing polymer particles, each decreasing the number of growing particles by one. Monomeric radicals ($M^{\bullet}$) are generated by chain transfer to monomer at a rate $k_{tr}C_{mon}^{(part)}N^*$, where k_{tr} is the bimolecular rate constant for chain transfer to monomer. A fraction (P_{prop}) of these continue propagating and do not change N^*. The other fraction terminates growing polymer particles, with each radical decreasing the number of growing particles by two. Clearly, the crucial parameter is the ratio p_{term}/p_{prop}. If p_{term}/p_{prop} is zero, eq 13 reduces to eq 5, which neglects termination of growing chains. A crude estimate for p_{term}/p_{prop} is simply

$$\frac{p_{term}}{p_{prop}} \approx \frac{\tau_{prop}}{\tau_{res}} \frac{N^*}{N} = \frac{1}{\tau_{res}k_pC_{mon}^{(mic)}} \frac{N^*}{N} \tag{15}$$

A more detailed derivation of the rate equation (14) starts from the coupled set of rate equations for the concentrations of aqueous phase free radicals, growing particles, and swollen micelles with adsorbed oligomeric free radicals, explicitly taking into account the adsorption−desorption process. In such a scheme it is easy to also include a possible difference in the adsorption rate constants of the oligomeric free radicals on particles and swollen micelles. As shown in Appendix A, this gives

$$\frac{p_{term}}{p_{prop}} = \frac{k_{ads}^{(part)}}{k_{ads}^{(mic)}} \frac{1}{\tau_{res}k_pC_{mon}^{(mic)}} \frac{N^*}{N} \tag{16}$$

For diffusion-controlled adsorption,

$$\frac{k_{ads}^{(part)}}{k_{ads}^{(mic)}} = \frac{R_{part}}{R_{mic}} \tag{17}$$

where R_{part} is the particle radius. For some small radicals, such as the initiator-derived radical species ($IM^{\bullet}$), the residence time in the growing particles may in fact be so small that the assumption of instantaneous termination is invalid. Hence, a further refinement of eq 16 could be necessary and would have to include an efficiency factor for the termination reaction.

Next we discuss the variation of p_{term}/p_{prop} as the reaction progresses. First consider the ratio $k_{ads}^{(part)}/k_{ads}^{(mic)} \approx R_{part}/R_{mic}$. During the reaction, the monomer swelling of both particles and micelles decreases. This implies that, to a first approximation, the ratio R_{part}/R_{mic} will be constant as the reaction proceeds. Therefore, in what follows, the ratio $k_{ads}^{(part)}/k_{ads}^{(part)}$ is assumed to be independent of conversion. While we do have an estimate for the residence time of the transfer-generated radicals, eq 12, there is no analogous estimate for the residence time of the initiator-derived free radicals that are surfactant-like. Specifically, there is no model for how the surfactant residence time depends on the radius of the microemulsion droplets. Nonetheless, the residence time is expected to scale with the water solubility of the initiator-derived radical ($IM^{\bullet}$), which in turn depends on the aqueous solubility of the monomer. Moreover, due to their higher rotational entropy, small free radicals are expected to have a higher reactivity compared to their polymeric counterparts. Effective k_p values approximately 4 times higher than the long-chain limit are expected on the basis of theoretical calculations.[19] Therefore, in what follows, we do not use a specific model for τ_{res} but instead simply assume that

$$\frac{p_{term}}{p_{prop}} = \frac{1}{\tau_{term}} \frac{1}{k_pC_{mon}^{(mic)}} \frac{N^*}{N} \tag{18}$$

where $\tau_{term} \approx \tau_{res}R_{mic}/R_{part}$ is a conversion-independent time scale into which the correction factor for k_p is invariably lumped. A final problem is that the relative contributions of the initiator-derived and the transfer-generated small free radicals to the termination process are unknown. Part of the problem is that, as mentioned, there is no detailed model for the residence time of the initiator-derived species ($IM_n^{\bullet}$). Therefore, in eq 14 we simply use a single value of p_{term}/p_{prop} or, equivalently, a single value of τ_{res} that characterizes the termination process. This parameter should be interpreted as a

characteristic residence time of the "typical" aqueous phase free radical that causes the termination.

According to eq 18, the ratio p_{term}/p_{prop} that enters the kinetic equations depends on the concentration of monomer in the micelles, as well as on the number density of micelles, both of which depend on the conversion. Given the monomer concentration in the polymer particles, for which we assume the functional form of eq 9, these quantities can be calculated using simple mass-balance equations. The explicit expressions for the micelle number density (N) and the concentration of monomer within them ($C_{mon}^{(mic)}$) are given in Appendix B.

Finally, within the context of the present model, we can interpret the assumption of Guo et al.,[5] that the rate constant for radical capture by the micelles, k_a' (using their notation), is many orders of magnitude smaller than that for capture by the particles, k_a. They attributed this to the fact that the micelles are highly charged. However, in the presence of so much surfactant the polymer particles are most likely fully covered with surfactant and hence are just as highly charged as the micelles. Even if this were not the case, electrostatics alone could not cause such a large difference in the capture rates of the small aqueous phase free radicals. This confusion arises because the process of radical capture by particles and micelles was not clearly defined. Radical capture by polymer particles affects the kinetics through bimolecular termination. This is a fast process; i.e., once a small free radical enters a growing particle, termination follows essentially immediately. On the other hand, radical capture by micelles represents the entire sequence of events up to the first propagation step in a monomer-swollen micelle, which is a slow process. Within the context of our theory, the ratio k_a/k_a', of the capture rate constants is simply

$$\frac{k_a}{k_a'} = \frac{k_{ads}^{(part)}}{k_{ads}^{(mic)}} \frac{\tau_{res}}{\tau_{prop}} \approx \frac{R_{part}}{R_{mic}} k_p C_{mon}^{(mic)} \tau_{res} \qquad (19)$$

which is indeed a large number, as found by Guo et al.[5]

3.3. Diffusion Limitations to Propagation. For polystyrene and poly(tC_4MA) that have glass transition temperatures of ~100 and ~115 °C, respectively,[20] diffusion limitations to propagation may arise within the polymer particles as the polymerization proceeds at 60 °C. Hence, we must address the question of whether this may also contribute to the shift in the location of the rate maxima to lower conversions. Note that the time scales for diffusion across the aqueous phase and the surfactant layers of the micelles and polymer particles are many orders of magnitude faster than the time scale of propagation and need no further consideration.[2]

For bulk radical polymerizations of styrene, Yamada et al.[21,22] have performed ESR measurements that led them to conclude that k_p is constant up to high conversions at 70 °C. However, qualitative reanalysis of their raw data indicate that a sharp drop in k_p is expected beyond 80% conversion.[21] Furthermore, their average molecular weights are very low[22] (M_n = 13 000 Da, M_w/M_n = 2.32 at 79% conversion) compared to the molecular weights (~10^7 Da) of polymers typically obtained from microemulsion polymerizations (part 3). Indeed, the glass transition temperature of polystyrene with M_n = 13 000 is only ~90 °C[23] compared to T_g ~ 100 °C for typical polystyrenes with M_n > 50 000.

Unfortunately, the decrease of k_p as a function of polymer content has not been measured for tC4MA. Nevertheless, by analogy with electron spin resonance (ESR) data for poly(methyl methacrylate) (T_g ~105 °C), as reviewed by Yamada et al.,[24] we expect that k_p should remain constant up to the volume fraction of polymer (~70%) where the polymer particles turn glassy.

From our monomer partitioning studies, the volume fraction of monomer in the polymer particles is ~30 vol % for both styrene and tC_4MA at their typical rate maxima at ~20% conversion. Given these results and the available literature data, it is unfortunately difficult to estimate the importance of diffusion limitations due to glass transition effects on the location of the rate maxima. In the absence of accurate data on the dependence of k_p on the polymer weight fraction for styrene or tC_4MA, we refrain from including this effect in our theory. Instead, we simply demonstrate the qualitative differences in the kinetic profiles for nC_4MA and tC_4MA which, recall, have essentially identical physical properties with the exception of their glass transition temperatures. From these observations, we then infer that diffusion limitations may combine with termination effects in shifting the maximum rate to ~20% conversion for styrene.

That diffusion limitations are the general cause for the decline in the propagation rate beyond the glass transition has been argued to be highly improbable by Faldi et al.[25] Their forced Rayleigh scattering and field-gradient NMR measurements of MMA diffusion coefficients in PMMA are 4 orders of magnitude greater than that necessary to achieve agreement with k_p values measured using ESR. Gilbert[26] compares these and other measurements of the diffusion coefficient with the value expected from ESR measurements of k_p in an emulsion polymerization as a function of polymer volume fraction in the particles. There is indeed a large difference between the diffusion coefficients calculated from k_p via the Smoluchowski equation and the direct diffusion coefficient measurements. However, as the diffusion coefficient measurements were performed on bulk mixtures of monomer and polymer while the diffusion coefficients calculated from ESR measurements of k_p were performed in an emulsion polymerization, the accuracy of such comparisons may be compromised by systematic errors in the measurement of polymer content. Gilbert's graphical comparison shows clearly that this discrepancy in the diffusion coefficients can be caused by small errors (~5%) in the measurement of the polymer volume fraction. As Faldi et al.[25] offer no alternative explanation for the generally observed decline in the propagation rate past the glass transition temperature, this apparent discrepancy is assumed to be due to experimental errors and will not be considered further.

4. Results and Discussion

4.1. C_6MA: Effect of Nonlinear Monomer Partitioning on Kinetics. We have previously studied the microemulsion polymerization kinetics of C_6MA with mixed DTAB/DDAB surfactants and found excellent agreement with our original kinetic model.[2] Here we simplify our model system by using only DTAB as the surfactant. To relate these new results to our previous kinetic studies, we first compare the microemulsion polymerization kinetics of the mixed microemulsions with that of microemulsions prepared with DTAB only.

This also allows us to study the influence that the surfactant has on the kinetics of microemulsion polymerization.

Figure 2 shows the conversion as a function of time for C_6MA/DTAB microemulsions initiated with V50 at 60 °C for two initiator concentrations. The conversion data are analyzed as described in section 2 to give the rate of polymerization as a function of conversion as shown in Figure 3.

Remarkably, a mere change of the surfactant mixture causes a shift in the location of the rate maximum from ~40% for the mixed DTAB/DDAB microemulsions down to about ~30% for the DTAB-only microemulsions. As discussed previously, the extent of radical termination is affected mainly by the physical properties of the monomer and initiator rather than by the properties of the microemulsion droplets. Hence, it is highly unlikely that a change of the surfactant mixture would invalidate the assumption of negligible termination that worked so well for the case of the mixed DTAB/DDAB microemulsions. More likely, the change in surfactant affects the microemulsion thermodynamics, i.e., monomer partitioning.

Recall that in the original kinetic model for the mixed microemulsions linear monomer partitioning was assumed. However, the measurements in part 1 show that the monomer partitioning for polymerizing C_6MA/DTAB microemulsions is significantly nonlinear ($b \approx 1.4$). Therefore, we hypothesize that the observed differences are caused by a difference in monomer partitioning. The mixed DTAB/DDAB system presumably has linear monomer partitioning, whereas the DTAB-only system has significantly nonlinear monomer partitioning, as measured experimentally. Unfortunately, it has not been possible to confirm that the monomer partitioning for the mixed DTAB/DDAB microemulsions is indeed linear. The reproducibility of SANS monomer partitioning studies for these microemulsions has so far been hampered by the tendency of C6MA latex particles to cream when prepared from DTAB/DDAB microemulsions in D_2O.

Despite this experimental difficulty, the expected difference in the monomer partitioning behavior of the mixed system as compared to the DTAB-only system can be explained using the thermodynamic model developed in part 1. This model, together with experimental monomer partitioning results for styrene, indicates that monomer partitioning becomes increasingly nonlinear close to the phase boundary. Indeed, on a surfactant-free basis, the DTAB-only microemulsion consists of $\alpha = 3$ wt % C_6MA, which is very close to the phase boundary that lies at $\alpha = 3.2$ wt %. Upon replacing 30% of the DTAB surfactant with DDAB to obtain the mixed system, the phase boundary shifts to $\alpha = 7.5$ wt %. Hence, it is likely there is a more linear monomer partitioning profile for our previous kinetic studies that were based on C_6MA/DTAB/DDAB microemulsions containing $\alpha = 5$ wt % monomer.

To demonstrate that nonlinear monomer partitioning is the cause of the observed differences, we compare our data with the modified kinetic model (eq 10) that still neglects biradical termination but accounts for nonlinear monomer partitioning. Theoretical curves for the kinetics are obtained by numerical integration of eq 10, using $b = 1.4$ as found experimentally. All parameters for the kinetic theory have been measured independently, except for the propagation rate constant of C_6MA. For the dissociation rate constant of the V50 initiator at 60 °C we use the value quoted by the manufacturer, $k_d = 3 \times 10^{-5}$ s^{-1}.[27] As for C_6MA/DTAB/DDAB microemulsion polymerization, aqueous phase termination is neglected, and an initiator efficiency of $\gamma_{eff} = 100\%$ is assumed. The monomer concentration initially present in the polymer particles was measured to be $C_{mon,0}^{(part)} = 2.96$ M in part 1. Finally, the macroscopic monomer concentration in the microemulsion was $M_0 = 0.18$ M. For the theoretical curves shown in Figures 2 and 3, a single value of $k_p = 940$ M^{-1} s^{-1} was used for the propagation rate constant. This value is perfectly consistent with the value of $k_p = 995$ M^{-1} s^{-1} that we have previously obtained by interpolating accurate pulsed-laser polymerization data for other linear alkyl methacrylates,[28] remembering that, for example, the value of the initiator decomposition rate constant is subject to considerable uncertainty.

The conversions at the maximum rate of polymerization are $f = 30 \pm 3\%$ and $f = 34 \pm 2\%$ respectively for the lowest and the highest value of the initiator concentration. To within experimental error, these measurements are in agreement with the theoretical value of 32% for $b = 1.4$ (see Table 2).

At higher conversions, the theoretical curves overestimate the rate of polymerization, especially for the lowest initiator concentration. This is similar to earlier measurements of the mixed surfactant microemulsions when compared to the previous kinetic model. Presumably, the deviations at higher conversions may be due to a small amount of termination, either in the aqueous phase or in the particles. As we have found for the case of C_6MA/DTAB/DDAB microemulsion polymerizations, in comparing the kinetic model to the experimental data, there is no way to accommodate low initiator efficiencies. In the present case, if we were to assume that initiation efficiencies are low due to some initial aqueous phase propagation, as suggested by the Maxwell−Morisson model[15] for entry in emulsion polymerization, our fitted values for k_p would have been unreasonably high.

4.2. Styrene: Effect of Termination and/or Diffusion Limitations on Kinetics. Next consider the polymerization kinetics of styrene. Figure 4 shows the conversion as a function of time for styrene/DTAB microemulsions containing $\alpha = 3$ wt % styrene initiated with V50 at 60 °C for three initiator concentrations. Again, the conversion data are analyzed as described in section 2 to give the rate of polymerization as a function of conversion, shown in Figure 5.

Consistent with data for styrene microemulsion polymerization obtained by others,[5,16,29−32] we find rate maxima at ~20% conversion. In part 1 of this series, we have measured highly linear monomer partitioning profiles for styrene/DTAB microemulsions containing $\alpha = 3$ wt % styrene. Therefore, the failure of the simple theory to account for the kinetics is presumably due to nonnegligible biradical termination and/or diffusion limitations to propagation.

While we have shown that significant aqueous phase termination is inconsistent with the observed kinetics of C_6MA, this is not necessarily true for styrene. The aqueous phase solubility of styrene (Table 1) is approximately 10 times higher than that of C_6MA while its propagation rate constant is only one-third that of C_6MA. These factors result in a much higher concentration of small styrene-based free radicals in the aqueous

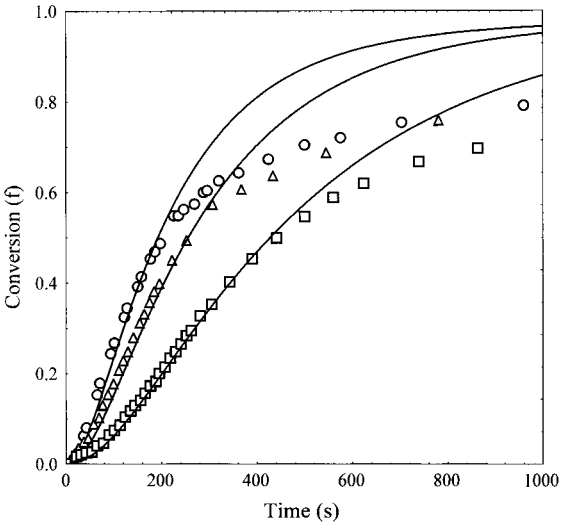

Figure 4. Experimental and model calculated kinetics for styrene/DTAB microemulsions containing $\alpha = 3$ wt % monomer on a surfactant-free basis. The microemulsions were initiated with (○) 0.49 mM, (△) 0.24 mM, and (□) 0.061 mM of V50 that correspond respectively to 0.5, 0.25, and 0.0625 wt % of the monomer in the microemulsion.

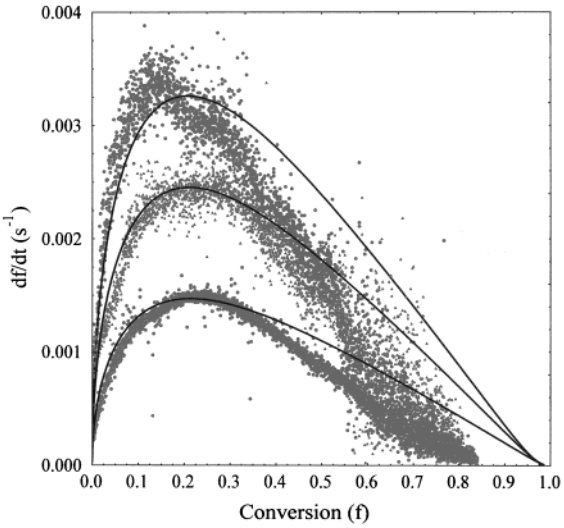

Figure 5. Experimental and model rate vs conversion profiles obtained by differentiating the data shown in Figure 4.

phase. Therefore, in comparing the data to our kinetic model, an initiation efficiency parameter (γ_{eff}) that accounts for possible aqueous phase termination is used. The only other unknown parameter is the characteristic time scale for termination ($\tau_{term} \approx \tau_{res} R_{mic}/R_{part}$), which is independent of the initiator concentration. The rate constant for chain transfer to monomer is not known to the same degree of accuracy as the propagation rate constant but is estimated to be about $k_{tr} = 0.02$ M^{-1} s^{-1}.[20] For the present styrene microemulsion composition, monomer partitioning is linear ($b \approx 1$) and the initial monomer concentration in the polymer particles is $C^{(part)}_{mon,0} = 1.67$ M (part 1). Finally, the macroscopic concentration of monomer in the microemulsion is $M_0 = 0.18$ M.

As shown in Figure 6, the position of the rate maximum in our kinetic model depends mainly on the value of the characteristic time scale for termination τ_{term} and is almost independent of the initiator concentration. Increasing the initiator concentration by a factor

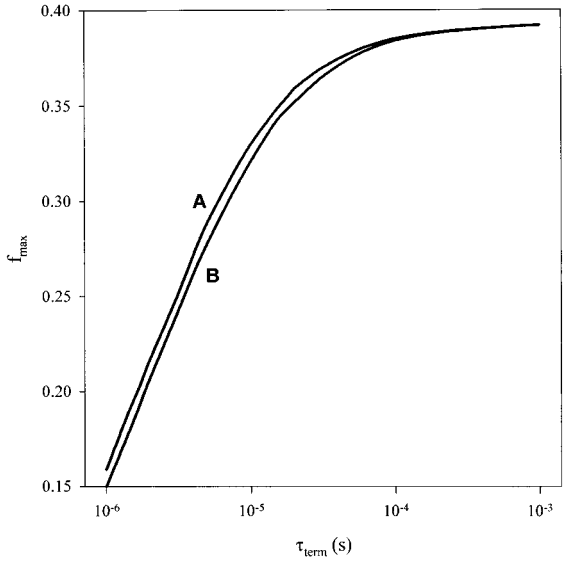

Figure 6. Model predicted variation of the conversion at the maximum rate of polymerization with respect to the characteristic time for termination (τ_{term}) for styrene/DTAB microemulsions containing $\alpha = 3$ wt % monomer. Curves A and B correspond to initiator radical fluxes of $\rho = 5 \times 10^{-9}$ M s^{-1} and $\rho = 5 \times 10^{-8}$ M s^{-1}, respectively.

of 10 shifts the predicted position of the maximum by only 1%. The positions of the rate maxima based on the experimental data in Figure 5 are at 16 ± 4%, 24 ± 5%, and 23 ± 2%, respectively, for decreasing initiator concentrations. From the average value of 21 ± 3%, the characteristic time scale for termination is estimated to be $\tau_{term} = (1.9 \pm 0.6) \times 10^{-6}$ s; that is consistent with the estimates described in section 3. The initiation efficiencies (γ_{eff}) are then estimated by fitting the experimental rate vs conversion data to the kinetic model. The solid curves in Figures 4 and 5 are the result of model calculations using $\tau_{term} = 1.9 \times 10^{-6}$ s and initiation efficiencies of 80%, 60%, and 55% for increasing initiator concentrations. At conversions beyond ~50%, the theoretical model overpredicts the polymerization rate. However, as the monomer partitioning measurements demonstrate (part 1), there is no doubt that diffusion limitations due to glass transition are important at such higher conversions.

The slight decrease of the initiation efficiencies with increasing initiator concentrations does indeed point to some aqueous phase termination. However, these high initiation efficiencies (55−80%) are clearly inconsistent with the aqueous phase chemistry suggested by the Maxwell−Morisson[15] model for radical entry in emulsion polymerizations. Assuming a critical degree of polymerization for entry of $z = 2$, the Maxwell−Morisson theory would predict extensive aqueous phase termination for styrene, leading to an initiation efficiency of only a few percent.

The microemulsions of interest here are concentrated dispersions of monomer-swollen micelles with intermicellar distances of ~10 nm.[4] Therefore, small free radicals in the aqueous phase are never further than a few nanometers from a monomer-swollen micelle. Moreover, for typical initiator concentrations of ~0.1 mM, the number of free radicals after characteristic reaction times of ~1000 s is only ~10^{-6} molecules/nm^3, 1000 times less than the number of micelles. Thus, aqueous free radicals in microemulsions encounter monomer much more frequently than they would when confined

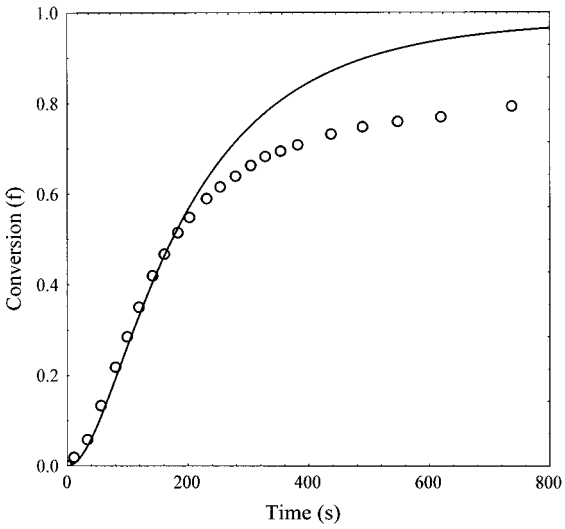

Figure 7. Experimental and model calculated kinetics for styrene/DTAB microemulsions containing $\alpha = 7$ wt % monomer on a surfactant-free basis. The microemulsion was initiated with (○) 0.57 mM of V50 that corresponds to 0.25 wt % of the amount of monomer in the microemulsion.

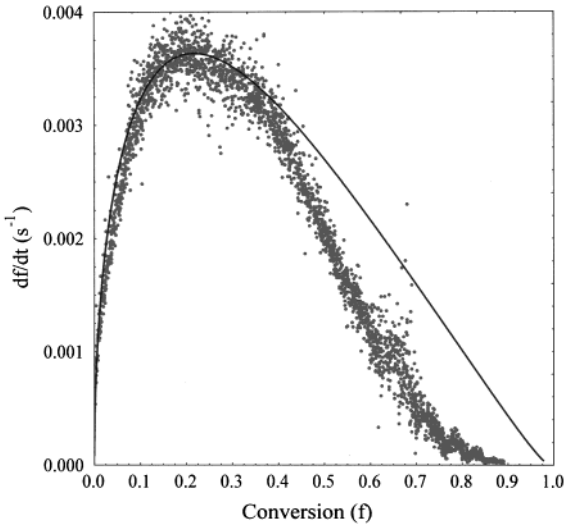

Figure 8. Experimental and model rate vs conversion profiles obtained by differentiating the data shown in Figure 7.

to the aqueous phase as assumed in the Maxwell–Morisson theory. Hence, we conclude that even for styrene microemulsion polymerization, radical capture by the monomer-swollen micelles is fast and aqueous phase termination is limited. Significantly, biradical termination can fully account for the position of the maximum rate of polymerization (~20%) for styrene microemulsions.

Up to this point, our analysis has ignored the possibility that the biradical termination effects we have just described may be simultaneously accompanied by diffusion limitations in determining the location of the rate maximum. To explore this possibility, we take advantage of the monomer partitioning measurements (part 1) for styrene/DTAB/D_2O microemulsions at higher monomer loadings. These measurements show that, for styrene/DTAB/D_2O microemulsions at $\alpha = 7.5$ wt %, the polymer particles contain at least 40 vol % of monomer up to 30% conversion. Thus, diffusion limitations cannot play a role in determining the location of the maximum polymerization rate for styrene/DTAB microemulsions close to the phase boundary, although they surely play a role at higher conversions.

Figures 7 and 8 show the kinetic profiles for a styrene/DTAB/H_2O microemulsion with $\alpha = 7$ wt %. The rate maximum, which still occurs at a low conversion of 21 ± 4%, corresponds to a characteristic time scale for termination of $\tau_{term} = (3-9) \times 10^{-6}$ s. An intermediate value of $\tau_{term} = 5 \times 10^{-6}$ s was used in conjunction with an initiation efficiency of 75% and $C_{mon,0}^{(part)} = 3.08$ M to calculate the solid curves shown in Figures 7 and 8. Observe that at conversion beyond ~50% the theoretical model again overpredicts the polymerization rate. As the monomer partitioning measurements (part 1) show, this observation is consistent with our rough estimate (~30 vol %) for the volume fraction of monomer in the polymer particles at which glass transition sets in. Note that the slight difference in the location of the phase boundary for styrene microemulsions made with H_2O and D_2O ($\alpha = 7.2$ and 8.2 wt %, respectively) is not expected to have a significant impact on monomer partitioning. Furthermore, as discussed in section 3.1, the nonlinear monomer partitioning at high styrene concentrations ($b = 1.4$) cannot lower the location of the maximum rate to below 30% conversion. From this result, we conclude that termination effects are important for styrene/DTAB microemulsion polymerizations.

Clearly, this description of the termination process is still highly approximate in the sense that the characteristic time scale for termination (τ_{term}) has been assumed to remain constant throughout the reaction and is equal for all species ($M^\bullet$ and $IM^\bullet$) involved. Aqueous phase termination has also been assumed to be independent of conversion even though the overall radical concentration increases with conversion. Furthermore, the possibility remains that termination effects may be accompanied by diffusion limitations to propagation for styrene/DTAB microemulsions at lower monomer loadings, e.g., the previous experiments performed at $\alpha = 3$ wt %. Nonetheless, this analysis is as complete as is warranted by the current experimental situation.

4.3. nC_4MA and tC_4MA: Effect of Diffusion Limitations Due to Glass Transition. DTAB-based microemulsions of nC_4MA and tC_4MA have physical properties that make them ideal model systems for probing the effects of diffusion limitations to propagation on the kinetics of microemulsion polymerizations. In part 1, we have shown that the monomer partitioning profiles for these butyl methacrylates are essentially identical. Moreover, as shown in Table 1, nC_4MA and tC_4MA have essentially identical water solubilities and propagation rate constants but polymer glass transition temperatures[20] that are respectively ~40 °C below and ~60 °C above the reaction temperature of 60 °C. This enables us to isolate the effects of glass transition and further explore the possibility that diffusion limitations accompany termination effects in setting the position of the maximum rate for styrene/DTAB microemulsions at low monomer loadings.

Figures 9 and 10 show the kinetic profiles for nC_4MA and tC_4MA microemulsions containing $\alpha = 3$ wt % of monomer initiated with V50 at 60 °C for two initiator concentrations. For nC_4MA, the maximum rate of polymerization occurs at 29 ± 6% and 27 ± 3% conversion. Similar to C_6MA/DTAB microemulsions, the shift in the position of the rate maximum from the theoretically predicted value of 39% down to an average of ~28% can be attributed mainly to nonlinear monomer partitioning

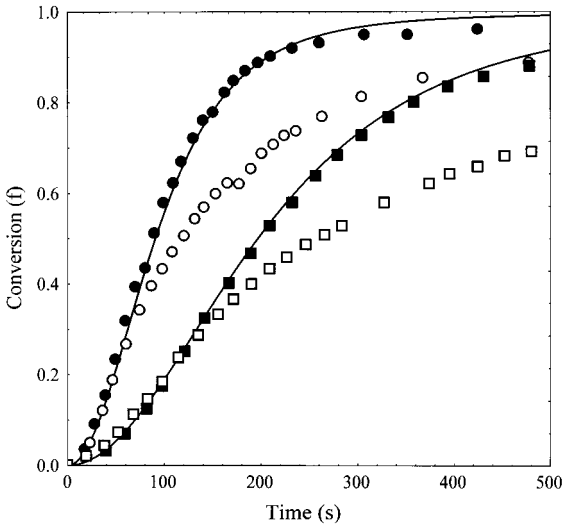

Figure 9. Experimental and model calculated kinetics for nC_4MA and tC_4MA DTAB-based microemulsions containing $\alpha = 3$ wt % monomer on a surfactant-free basis. The microemulsions were initiated with V50: (●: nC_4MA, 0.24 mM; ■: nC_4MA, 0.061 mM) and (○: tC_4MA, 0.24 mM; □: tC_4MA, 0.061 mM). These initiator concentrations correspond to 0.25 and 0.625 wt % of the monomer.

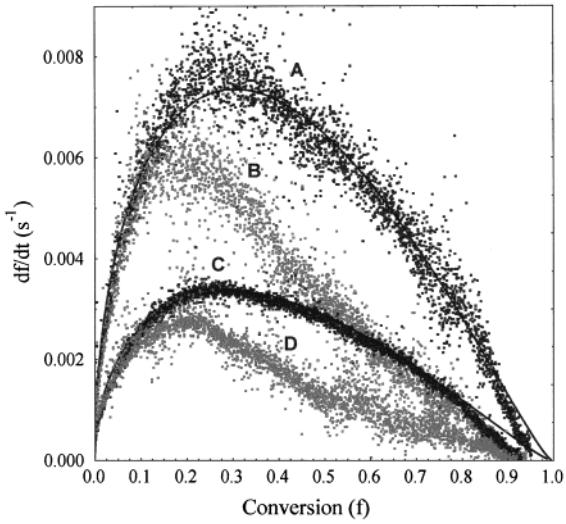

Figure 10. Experimental and model rate vs conversion profiles obtained by differentiating the data shown in Figure 9 (A: nC_4MA, 0.24 mM; C: nC_4MA, 0.061 mM) and (B: tC_4MA, 0.24 mM; D: tC_4MA, 0.061 mM).

($b = 1.4$). Interestingly, even though nC_4MA has the same aqueous solubility as styrene, which is approximately 10 times higher than that of C_6MA (Table 1), termination effects remain negligible. Indeed, the solid curves in Figures 9 and 10 are the result of model calculations obtained by conservatively assuming the same value for the characteristic time scale for termination ($\tau_{term} = (1.9 \pm 0.6) \times 10^{-6}$ s) as that for styrene/DTAB microemulsions at $\alpha = 3$ wt %. A literature value of $k_{tr} = 0.02$ M^{-1} s^{-1},[20] equal to that for styrene, was also used for the chain-transfer constant of nC_4MA monomer. Recall that these values for τ_{term} and k_{tr} fully accounted for the shift in the maximum rate to ~20% conversion for styrene/DTAB microemulsion with $\alpha = 3$ wt %. Furthermore, note that unlike the present nC_4MA microemulsions, for which nonlinear monomer partitioning alone would have shifted the maximum rate to 32% conversion (Table 2), the styrene microemulsions exhibited linear monomer partitioning ($b = 1$). Apparently, the higher propagation rate constant of nC_4MA[28] compared to styrene (1015 vs 342 M^{-1} s^{-1}) is adequate to compensate for its high water solubility. Moreover, the value now quoted for τ_{term} of styrene/DTAB microemulsions at $\alpha = 3$ wt % was obtained assuming that diffusion limitations to propagation are absent.

Ultimately, however, the most interesting feature of Figures 9 and 10 is the manner in which the kinetic profiles of nC_4MA and tC_4MA track each other. As expected, due to their similar physical properties, the kinetic profile of tC_4MA matches that of nC_4MA up to ~15% conversion after which it begins to fall below. This eventually leads to maximum rates of polymerization at 19 ± 5% and 20 ± 3% conversion for tC_4MA. Following our previous discussion, we can only conclude that the drop in the rate of tC_4MA polymerizations is due to diffusion limitations resulting from a glass transition. This result suggests that diffusion limitations may also be important for styrene microemulsion polymerizations with low monomer content.

However, it is not very reassuring to note that our monomer partitioning measurements (part 1) indicate that up to 35 vol % of tC_4MA is still present in the polymer particles at 15% conversion. As mentioned previously, ESR measurements[24] for poly(methyl methacrylate) show that propagation becomes diffusion limited only at monomer volume fractions less than 30%. Nevertheless, there remains the remote possibility that nascent poly(tC_4MA) or polystyrene particles become glassy at their earliest stages of growth. If this is true, monomer partitioning to the propagating particles may be diffusion-controlled. Unfortunately, the SANS monomer partitioning measurements offer no insight into this issue because it is not possible to isolate the growing particles that constitute only a small fraction of the total number of polymer particles.

5. Conclusions

Application of our monomer partitioning results (part 1) to the polymerization kinetics of C_6MA and nC_4MA DTAB-based microemulsions highlights the effect of nonlinear monomer partitioning on the location of the maximum rate of polymerization. For microemulsion compositions approaching the phase boundary, increasingly nonlinear monomer partitioning shifts the maximum rate from a predicted value of 39% conversion for linear monomer partitioning to lower conversions of ~30%. Nonlinear monomer partitioning cannot account for the low conversions (~20%) at which the maximum rate has been observed for styrene. A more careful, albeit still approximate, analysis demonstrates that, in contradiction to the assumptions of our original kinetic model, biradical termination effects cannot be readily dismissed. Although biradical termination is indeed negligible for C_6MA and nC_4MA, and presumably for tC_4MA as well, it is the dominant mechanism that establishes the location of the maximum rate for styrene. The relative importance of termination is determined to a large extent by the water solubility and reactivity of the monomer. In going from C_6MA to styrene, the 10-fold increase in monomer water solubility and 3-fold reduction in the propagation rate constant drastically increases the possibility of small free radicals encountering and terminating growing polymer particles. Up to this point, there is still no direct evidence for the role of glass transition during styrene micro-

emulsion polymerizations, and its effect is still uncertain. Nevertheless, the startling similarities and differences in the kinetic profiles of nC_4MA and tC_4MA lead us to believe that diffusion limitations may also play an important, yet so far unclear, mechanistic role during styrene microemulsion polymerizations.

Appendix A

Here we derive eq 16 for p_{term}/p_{prop} using a coupled set of rate equations for the concentration of aqueous phase free radicals (N^*_{aq}), the concentration of growing particles (N^*), and the concentration of swollen micelles with adsorbed oligomeric free radicals (N^*_{aq}). The equations below are very similar to those for the fate of transfer-generated radicals in emulsion polymerization, as discussed by Gilbert.[26] To derive eq 16, it is sufficient to consider only initiator-derived oligomeric free radicals. Also, aqueous phase termination is not taken into account here. The extensions to also include transfer-generated radicals and aqueous phase termination are straightforward but more involved and lead to the same result for p_{term}/p_{prop}.

Oligomeric aqueous phase radicals are generated at a rate ρ_0 and adsorb on monomer-swollen micelles or growing particles. Adsorption by dead particles is neglected. The second-order rate constants for adsorption on micelles and particles are respectively $k_{ads}^{(mic)}$ and $k_{ads}^{(part)}$. Adsorption on a growing particle leads to instantaneous termination, but oligomeric radicals adsorbed on micelles desorb back to the aqueous phase at a rate $k_{des}^{(mic)}$:

$$\frac{\partial N^*_{aq}}{\partial t} = \rho_0 - k_{ads}^{(mic)} N N^*_{aq} - k_{ads}^{(part)} N^* N^*_{aq} + k_{des}^{(mic)} N^*_{mic} \tag{A1}$$

where N is the concentration of monomer-swollen micelles. Either micelles with adsorbed oligomeric free radicals lose the radical through desorption, or the radical propagates and becomes a growing particle:

$$\frac{\partial N^*_{mic}}{\partial t} = k_{ads}^{(mic)} N N^*_{aq} - k_{des}^{(mic)} N^*_{mic} - k_p C_{mon}^{(mic)} N^*_{mic} \tag{A2}$$

Finally, the rate equation for the concentration of growing particles is

$$\frac{\partial N^*}{\partial t} = k_p C_{mon}^{(mic)} N^*_{mic} - k_{ads}^{(part)} N^*_{aq} N^* \tag{A3}$$

The adsorption−desorption process is fast on the time scale of the polymerization reaction. Hence, we can use the steady-state approximation to calculate the concentrations of aqueous phase free radicals and micelles with adsorbed oligomeric free radicals from eqs A1 and A2. At this stage it is convenient to introduce the small dimensionless quantities r_1 and r_2,

$$r_1 = \frac{k_{ads}^{(part)}}{k_{ads}^{(mic)}} \frac{N^*}{N} \tag{A4}$$

$$r_2 = \frac{k_p C_{mon}^{(mic)}}{k_{des}^{(mic)}} \tag{A5}$$

In terms of these quantities, the steady-state results for N^*_{aq} and N^*_{mic} are

$$N^*_{aq} = \frac{\rho_0}{k_{ads}^{(mic)} N} \frac{1 + r_1}{(1 + r_1)(1 + r_2) - 1} \approx \frac{\rho_0}{k_{ads}^{(mic)} N} \frac{1}{r_1 + r_2} \tag{A6}$$

$$N^*_{mic} = \frac{\rho_0}{k_{des}^{(mic)}} \frac{1}{(1 + r_1)(1 + r_2) - 1} \approx \frac{\rho_0}{k_{des}^{(mic)}} \frac{1}{r_1 + r_2} \tag{A7}$$

Substituting these expressions in the rate equation for the concentration of growing particles, eq A3, one finds

$$\frac{\partial N^*}{\partial t} = \rho_0 \frac{1 - r_1/r_2}{1 + r_1/r_2} \tag{A8}$$

Hence we identify

$$\frac{p_{term}}{p_{prop}} = \frac{r_1}{r_2} = \frac{k_{ads}^{(part)}}{k_{ads}^{(mic)}} \frac{k_{des}^{(mic)}}{k_p C_{mon}^{(mic)}} \frac{N^*}{N} \tag{A9}$$

This is identical to eq 16 upon setting $k_{des}^{(mic)} = 1/\tau_{res}$.

Appendix B

Explicit expressions for the monomer concentration in the micelles ($C_{mon}^{(mic)}$) and for the concentration of micelles (N) can be deduced from the monomer concentration in the particles (eq 8) through mass balance equations. The composition of the initial microemulsion is set by the initial volume fraction of monomer ($\phi_{mon,0}$) and by the surfactant volume fraction (ϕ_{surf}). Following the analysis in part 1, the monomer and polymer volume fractions during the polymerization reaction are approximated by

$$\phi_{mon} = (1 - f)\phi_{mon,0} \tag{B1}$$

$$\phi_{pol} = f\phi_{mon,0} \tag{B2}$$

The monomer partitions between particles and micelles:

$$\phi_{mon} = \phi_{mon}^{(mic)} + \phi_{mon}^{(part)} \tag{B3}$$

Again following our previous paper on monomer partitioning, the extent of swelling of the micelles is characterized by the parameter

$$x \equiv \frac{R_{mic}}{R_{mic,0}} = 1 + \frac{\phi_{mon}^{(mic)}}{\phi_{surf}} \tag{B4}$$

where $R_{mic,0}$ is the radius of the empty micelles, at zero monomer content, and where we assume that the surfactant headgroup area does not depend on the extent of swelling of the micelles. The swelling of the polymer particles is characterized by their monomer volume fraction,

$$\nu_{mon} = \frac{\phi_{mon}^{(part)}}{\phi_{mon}^{(part)} + \phi_{pol}} \tag{B5}$$

This is related to the monomer concentration in the particles by $C_{mon}^{(part)} = C_{mon}\nu_{mon}$, where C_{mon} is the concentration of pure monomer. Neglecting the small amount of surfactant that is adsorbed on the particles,

the two swelling parameters are related by the mass balance equation

$$x = 1 + \frac{\phi_{\mathrm{mon},0}}{\phi_{\mathrm{surf}}}\left(1 - \frac{f}{1 - \nu_{\mathrm{mon}}}\right) \qquad \text{(B6)}$$

The above expressions directly relate the concentration of monomer in the micelles,

$$C_{\mathrm{mon}}^{(\mathrm{mic})} = C_{\mathrm{mon}} \frac{\phi_{\mathrm{mon}}^{(\mathrm{mic})}}{\phi_{\mathrm{mon}}^{(\mathrm{mic})} + \phi_{\mathrm{surf}}} = C_{\mathrm{mon}}(1 - 1/x) \qquad \text{(B7)}$$

and the concentration of monomer-swollen micelles

$$N = \frac{\phi_{\mathrm{mon}}^{(\mathrm{mic})} + \phi_{\mathrm{surf}}}{\frac{4}{3}\pi R_{\mathrm{mic}}^3} = \frac{\phi_{\mathrm{surf}}}{\frac{4}{3}\pi R_{\mathrm{mic},0}^3} \frac{1}{x^2} \qquad \text{(B8)}$$

to the monomer concentration in the particles, the composition variables $\phi_{\mathrm{mon},0}$ and ϕ_{surf} of the initial microemulsion, and to the extent of conversion.

References and Notes

(1) Lusvardi, K. M.; Schubert, K. V.; Kaler, E. W. *Langmuir* **1995**, *11*, 4728.
(2) Morgan, J. D.; Lusvardi, K. M.; Kaler, E. W. *Macromolecules* **1997**, *30*, 1897.
(3) Morgan, J. D.; Kaler, E. W. *Macromolecules* **1998**, *31*, 3197.
(4) Co, C. C.; Kaler, E. W. *Macromolecules* **1998**, *31*, 3203.
(5) Guo, J. S.; Sudol, E. D.; Vanderhoff, J. W.; El-Aasser, M. S. *J. Polym. Sci., Polym. Chem.* **1992**, *30*, 703.
(6) Mendizabal, E.; Flores, J.; Puig, J. E.; Lopez-Serrano, F.; Alvarez, J. *Eur. Polym. J.* **1998**, *34*, 411.
(7) Behrman, E. J.; Edwards, J. O. *Rev. Inorg. Chem.* **1980**, *2*, 179.
(8) Craven, P.; Wahba, G. *Numer. Math.* **1979**, *31*, 377.
(9) Efron, B.; Tibshirani, R. *Stat. Sci.* **1986**, *1*, 54.
(10) Lane, W. H. *Ind. Eng. Chem.* **1946**, *18*, 295.
(11) Halnan, L. F.; Napper, D. H.; Gilbert, R. G. *J. Chem. Soc., Faraday Trans. 1* **1984**, *80*, 2851.
(12) Yalkowsky, S. H.; Banerjee, S. *Aqueous Solubility: Methods of Estimation for Organic Compounds*; Marcel Dekker: New York, 1992.
(13) Quian, R.; Wu, L.; Shen, D.; Napper, D. H.; Mann, R. A.; Sangster, D. F. *Macromolecules* **1993**, *26*, 2950.
(14) McAskill, N. A.; Sangster, D. F. *Aust. J. Chem.* **1979**, *32*, 2611.
(15) Maxwell, I. A.; Morrison, B. R.; Napper, D. H.; Gilbert, R. G. *Macromolecules* **1991**, *24*, 1629.
(16) Full, A. P.; Kaler, E. W.; Arellano, J.; Puig, J. E. *Macromolecules* **1996**, *29*, 2764.
(17) Capek, I.; Juranicova, V. *Eur. Polym. J.* **1998**, *34*, 783.
(18) Full, A. P.; Puig, J. E.; Gron, L. U.; Kaler, E. W.; Minter, J. R.; Mourey, T. H.; Texter, J. *Macromolecules* **1992**, *25*, 5157.
(19) Gilbert, R. G.; Smith, S. C. *Theory of Unimolecular and Recombination Reactions*; Blackwell Scientific: Oxford, 1990.
(20) *Polymer Handbook*, 3rd ed.; Brandrup, J., Immergut, E. H., Eds.; John Wiley & Sons: New York, 1989.
(21) Yamada, B.; Kageoka, M.; Takayuki, O. *Macromolecules* **1991**, *24*, 5234.
(22) Yamada, B.; Kageoka, M.; Otsu, T. *Polym. Bull.* **1992**, *28*, 75.
(23) O'Driscoll, K.; Amin Sanayei, R. *Macromolecules* **1991**, *24*, 4479.
(24) Yamada, B.; Westmoreland, D. G.; Kobatake, S.; Konosu, O. *Prog. Polym. Sci.* **1999**, *24*, 565.
(25) Faldi, A.; Tirrell, M.; Lodge, T. P.; Vonmeerwall, E. *Macromolecules* **1994**, *27*, 4184.
(26) Gilbert, R. G. *Emulsion Polymerization: A Mechanistic Approach*; Academic Press: San Diego, 1995.
(27) *V-50*; Wako Pure Chemical Industries, Ltd.: Richmond, VA.
(28) Hutchinson, R. A.; Beuermann, S.; Paquet, D. A., Jr.; McMinn, J. H. *Macromolecules* **1997**, *30*, 3490.
(29) Guo, J. S.; El-Aasser, M. S.; Vanderhoff, J. W. *J. Polym. Sci., Polym. Chem.* **1989**, *27*, 691.
(30) Perez-Luna, V. H.; Puig, J. E.; Castano, V. M.; Rodriguez, B. E.; Murthy, A. K.; Kaler, E. W. *Langmuir* **1989**, *6*, 1040.
(31) Guo, J. S.; Sudol, E. D.; Vanderhoff, J. W.; El-Aasser, M. S. *J. Polym. Sci., Polym. Chem. Ed.* **1992**, *30*, 691.
(32) Nomura, M.; Suzuki, K. *Macromol. Chem. Phys.* **1997**, *198*, 3025.
(33) Pascal, P.; Winnik, M. *Makromol. Chem., Rapid Commun.* **1993**, *14*, 213.
(34) Deady, M.; Mau, A. W. H.; Moad, G.; Spurling, T. H. *Makromol. Chem.* **1993**, *194*, 1691.
(35) Hutchinson, R. A.; Aronson, M. T.; Richards, J. R. *Macromolecules* **1993**, *26*, 6410.

MA001247J